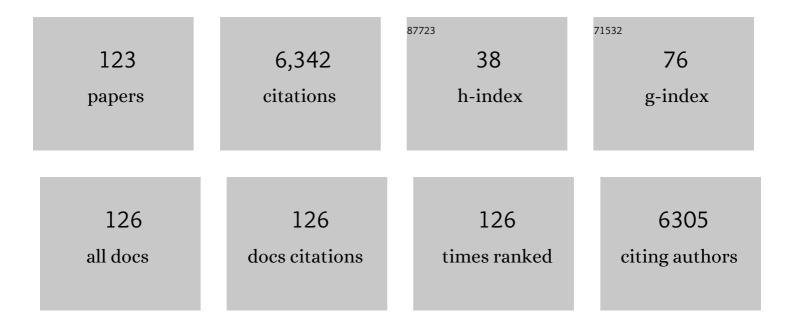
List of Publications by Year in descending order

Source: https://exaly.com/author-pdf/5733800/publications.pdf Version: 2024-02-01



ILARIN LILL

#	Article	IF	CITATIONS
1	Enhanced strength and ductility in a high-entropy alloy via ordered oxygen complexes. Nature, 2018, 563, 546-550.	13.7	988
2	Evading the strength–ductility trade-off dilemma in steel through gradient hierarchical nanotwins. Nature Communications, 2014, 5, 3580.	5.8	739
3	Structural Directed Growth of Ultrathin Parallel Birnessite on β-MnO ₂ for High-Performance Asymmetric Supercapacitors. ACS Nano, 2018, 12, 1033-1042.	7.3	436
4	Enhancement of strength-ductility trade-off in a high-entropy alloy through a heterogeneous structure. Acta Materialia, 2019, 165, 444-458.	3.8	336
5	Stacking fault energy of face-centered-cubic high entropy alloys. Intermetallics, 2018, 93, 269-273.	1.8	312
6	Ultralarge elastic deformation of nanoscale diamond. Science, 2018, 360, 300-302.	6.0	208
7	Construction of rGO wrapping octahedral Ag-Cu2O heterostructure for enhanced visible light photocatalytic activity. Applied Catalysis B: Environmental, 2018, 227, 132-144.	10.8	131
8	Nanoprecipitates induced dislocation pinning and multiplication strategy for designing high strength, plasticity and conductivity Cu alloys. Scripta Materialia, 2021, 195, 113741.	2.6	103
9	Local chemical fluctuation mediated ductility in body-centered-cubic high-entropy alloys. Materials Today, 2021, 46, 28-34.	8.3	98
10	Deformation twinning behaviors of the low stacking fault energy high-entropy alloy: An in-situ TEM study. Scripta Materialia, 2017, 137, 9-12.	2.6	90
11	Transformation-reinforced high-entropy alloys with superior mechanical properties via tailoring stacking fault energy. Journal of Alloys and Compounds, 2019, 792, 444-455.	2.8	90
12	Gradient twinned 304 stainless steels for high strength and high ductility. Materials Science & Engineering A: Structural Materials: Properties, Microstructure and Processing, 2016, 667, 179-188.	2.6	87
13	In situ growth of FeS microsheet networks with enhanced electrochemical performance for lithium-ion batteries. Journal of Materials Chemistry A, 2015, 3, 8742-8749.	5.2	86
14	High-order hierarchical nanotwins with superior strength and ductility. Acta Materialia, 2018, 149, 397-406.	3.8	85
15	Nonbasal Slip Systems Enable a Strong and Ductile Hexagonal-Close-Packed High-Entropy Phase. Physical Review Letters, 2019, 122, 075502.	2.9	83
16	Improvement of mechanical behaviors of a superlight Mg-Li base alloy by duplex phases and fine precipitates. Journal of Alloys and Compounds, 2018, 735, 2625-2633.	2.8	80
17	<i>In Situ</i> TEM on the Reversibility of Nanosized Sn Anodes during the Electrochemical Reaction. Chemistry of Materials, 2014, 26, 4102-4108.	3.2	79
18	Microstructure evolution and properties of Cu–Ag microcomposites with different Ag content. Materials Science & Engineering A: Structural Materials: Properties, Microstructure and Processing, 2006, 435-436, 237-244.	2.6	78

#	Article	IF	CITATIONS
19	Dislocation activities at the martensite phase transformation interface in metastable austenitic stainless steel: An in-situ TEM study. Materials Science & Engineering A: Structural Materials: Properties, Microstructure and Processing, 2017, 703, 236-243.	2.6	78
20	Solving the strength-ductility tradeoff in the medium-entropy NiCoCr alloy via interstitial strengthening of carbon. Intermetallics, 2019, 106, 77-87.	1.8	77
21	Approaching diamond's theoretical elasticity and strength limits. Nature Communications, 2019, 10, 5533.	5.8	73
22	Spatially-confined lithiation–delithiation in highly dense nanocomposite anodes towards advanced lithium-ion batteries. Energy and Environmental Science, 2015, 8, 1471-1479.	15.6	69
23	High strength and high conductivity Cu alloys: A review. Science China Technological Sciences, 2020, 63, 2505-2517.	2.0	60
24	Template-directed synthesis of pyrite (FeS ₂) nanorod arrays with an enhanced photoresponse. Journal of Materials Chemistry A, 2014, 2, 9496-9505.	5.2	58
25	Impacts of atomic scale lattice distortion on dislocation activity in high-entropy alloys. Extreme Mechanics Letters, 2017, 17, 38-42.	2.0	52
26	Influence of heat-treatment on the dynamic behavior of 3D laser-deposited Ti–6Al–4V alloy. Materials Science & Engineering A: Structural Materials: Properties, Microstructure and Processing, 2016, 677, 153-162.	2.6	50
27	Carbon coating may expedite the fracture of carbon-coated silicon core–shell nanoparticles during lithiation. Nanoscale, 2016, 8, 5254-5259.	2.8	50
28	In-situ TEM study of the dynamic interactions between dislocations and precipitates in a Cu-Cr-Zr alloy. Journal of Alloys and Compounds, 2018, 765, 560-568.	2.8	48
29	Direct Observation of Room-Temperature Dislocation Plasticity in Diamond. Matter, 2020, 2, 1222-1232.	5.0	48
30	Atomic deformation mechanism and interface toughening in metastable high entropy alloy. Materials Today, 2020, 37, 64-73.	8.3	48
31	Nature-Inspired Hierarchical Steels. Scientific Reports, 2018, 8, 5088.	1.6	47
32	Atomistic simulation for deforming complex alloys with application toward TWIP steel and associated physical insights. Journal of the Mechanics and Physics of Solids, 2017, 98, 290-308.	2.3	46
33	Alignment-controlled hydrothermal growth of well-aligned ZnO nanorod arrays. Journal of Physics and Chemistry of Solids, 2014, 75, 808-817.	1.9	44
34	Strength gradient enhances fatigue resistance of steels. Scientific Reports, 2016, 6, 22156.	1.6	43
35	Effects of Cr addition on the microstructural, mechanical and electrical characteristics of Cu–6wt.%Ag microcomposite. Scripta Materialia, 2005, 52, 587-592.	2.6	42
36	Microstructure evolution of Cu/Ag interface in the Cu–6 wt.% Ag filamentary nanocomposite. Acta Materialia, 2011, 59, 1191-1197.	3.8	41

#	Article	IF	CITATIONS
37	Machine learning-assisted discovery of strong and conductive Cu alloys: Data mining from discarded experiments and physical features. Materials and Design, 2021, 197, 109248.	3.3	41
38	Effects of Cr and Zr additions on the microstructure and properties of Cu–6wt.% Ag alloys. Materials Science & Engineering A: Structural Materials: Properties, Microstructure and Processing, 2012, 532, 331-338.	2.6	40
39	In situ tem investigation on ultrafast reversible lithiation and delithiation cycling of Sn@C yolk-shell nanoparticles as anodes for lithium ion batteries. Nano Energy, 2017, 40, 187-194.	8.2	38
40	Epitaxial TiO2/SnO2 core–shell heterostructure by atomic layer deposition. Journal of Materials Chemistry, 2012, 22, 10665.	6.7	34
41	Thickness-dependent fracture of amorphous carbon coating on SnO 2 nanowire electrodes. Carbon, 2014, 80, 793-798.	5.4	34
42	Interface structure and energy in Cu–71.8wt.% Ag. Journal of Alloys and Compounds, 2008, 464, 168-173.	2.8	31
43	In-situ TEM study of the lithiation and delithiation of FeS nanosheets. Journal of Alloys and Compounds, 2016, 688, 946-952.	2.8	31
44	Homogeneous arc ablation behaviors of CuCr cathodes improved by chromic oxide. Journal of Materials Science and Technology, 2021, 81, 1-12.	5.6	31
45	In situ TEM study on crack propagation in nanoscale Au thin films. Scripta Materialia, 2011, 65, 377-379.	2.6	30
46	Surface nanocrystallization of Mg-3 wt.% Li-6 wt.% Al alloy by surface mechanical attrition treatment. Materials Characterization, 2016, 120, 124-128.	1.9	28
47	Dislocation Strengthening without Ductility Trade-off in Metastable Austenitic Steels. Scientific Reports, 2016, 6, 35345.	1.6	27
48	Pulsed laser deposited NiO–NiSe nanocomposite as a new anode material for lithium storage. Journal of Alloys and Compounds, 2016, 661, 190-195.	2.8	27
49	Strengthening Effect of Ag Precipitates in Cu–Ag Alloys: A Quantitative Approach. Materials Research Letters, 2016, 4, 37-42.	4.1	25
50	Rare earth microalloying in as-cast and homogenized alloys Cu–6wt.% Ag and Cu–24wt.% Ag. Journal of Alloys and Compounds, 2006, 425, 185-190.	2.8	24
51	Effects of rare-earth additions on the microstructure and strength of Cu–Ag composites. Materials Science & Engineering A: Structural Materials: Properties, Microstructure and Processing, 2008, 498, 392-396.	2.6	24
52	Development of high-performance cathode catalyst of polypyrrole modified carbon supported CoOOH for direct borohydride fuel cell. Journal of Power Sources, 2017, 339, 13-19.	4.0	24
53	Carbon supported silver nanowires with enhanced catalytic activity and stability used as a cathode in a direct borohydride fuel cell. Journal of Materials Chemistry A, 2013, 1, 15323.	5.2	23
54	Improved strength and enhanced pitting corrosion resistance of Al-Mn alloy with Zr addition. Materials Letters, 2019, 255, 126535.	1.3	22

#	Article	IF	CITATIONS
55	Hexagonal Closed-Packed Precipitation Enhancement in a NbTiHfZr Refractory High-Entropy Alloy. Metals, 2019, 9, 485.	1.0	22
56	Crystal structure and morphology of a rare-earth compound in Cu–12wt.% Ag. Journal of Alloys and Compounds, 2009, 468, 73-76.	2.8	21
57	CoTi precipitates: The key to high strength, high conductivity and good softening resistance in Cu-Co-Ti alloy. Materials Characterization, 2021, 176, 111099.	1.9	21
58	Excellent thermal shock resistance of NiCrAlY coatings on copper substrate via laser cladding. Journal of Materials Science and Technology, 2022, 130, 93-102.	5.6	21
59	Adiabatic shear localization in nanostructured face centered cubic metals under uniaxial compression. Materials and Design, 2016, 105, 262-267.	3.3	20
60	In-situ high throughput synthesis of high-entropy alloys. Scripta Materialia, 2019, 160, 44-47.	2.6	20
61	Electrical failure behaviors of semiconductor oxide nanowires. Nanotechnology, 2011, 22, 405703.	1.3	19
62	High electrocatalytic activity for borohydride oxidation on palladium nanocubes enclosed by {200} facets. Journal of Power Sources, 2015, 299, 241-245.	4.0	18
63	Preparation of FeS2 nanotube arrays based on layer-by-layer assembly and their photoelectrochemical properties. Materials Science and Engineering B: Solid-State Materials for Advanced Technology, 2016, 204, 38-44.	1.7	18
64	Vacancy-assisted oxygen reduction reaction on cobalt-based catalysts in direct borohydride fuel cell revealed by in-situ XAFS and XRD. Electrochimica Acta, 2017, 254, 72-78.	2.6	18
65	Microstructure and hardness evolution during isothermal process at 700°C for Fe–24Mn–0.7Si–1.0Al TWIP steel. Materials Characterization, 2010, 61, 1356-1358.	1.9	17
66	Atomic Structure of Polypyrrole-Modified Carbon-Supported Cobalt Catalyst. Journal of Physical Chemistry C, 2012, 116, 20225-20229.	1.5	17
67	Superior flexibility of a wrinkled carbon shell under electrochemical cycling. Journal of Materials Chemistry A, 2014, 2, 4192.	5.2	17
68	Construction of FeS ₂ â€Sensitized ZnO@ZnS Nanorod Arrays with Enhanced Optical and Photoresponse Performances. Advanced Materials Interfaces, 2015, 2, 1500163.	1.9	17
69	Introducing catalyst in alkaline membrane for improved performance direct borohydride fuel cells. Journal of Power Sources, 2018, 374, 113-120.	4.0	17
70	Evolution of FCC/BCC interface and its effect on the strengthening of severe drawn Cu–3wt.% Cr. Journal of Alloys and Compounds, 2015, 640, 45-50.	2.8	16
71	Co-deformation in Cu–6wt.% Ag nanocomposites. Scripta Materialia, 2011, 64, 665-668.	2.6	15
72	Synthesis of fluorine-doped <i>α</i> -Fe ₂ O ₃ nanorods toward enhanced lithium storage capability. Nanotechnology, 2017, 28, 065401.	1.3	15

#	Article	IF	CITATIONS
73	Microstructure and hardness of Cu-12% Fe composite at different drawing strains. Journal of Zhejiang University: Science A, 2014, 15, 149-156.	1.3	14
74	Atomic resolution observation of conversion-type anode RuO ₂ during the first electrochemical lithiation. Nanotechnology, 2015, 26, 125404.	1.3	14
75	Trace bis-(3-sulfopropyl)-disulfide enhanced electrodeposited copper foils. Journal of Materials Science and Technology, 2021, 74, 237-245.	5.6	14
76	He-enhanced heterogeneity of radiation-induced segregation in FeNiCoCr high-entropy alloy. Journal of Materials Science and Technology, 2022, 101, 226-233.	5.6	14
77	W–Cu/Cu composite electrodes fabricated via laser surface alloying. Materials Characterization, 2022, 185, 111715.	1.9	14
78	Relationships between mechanical strength and electrical conductivity for Cu–Ag filamentary microcomposites. Applied Physics A: Materials Science and Processing, 2007, 86, 529-532.	1.1	13
79	Functionalization of polyvinyl alcohol composite membrane by CoOOH for direct borohydride fuel cells. Electrochemistry Communications, 2017, 77, 1-4.	2.3	13
80	Alter martensitic phase transformation kinetics by forming Ni-rich nanolayer in metastable austenitic steels. Science China Technological Sciences, 2019, 62, 546-550.	2.0	13
81	Effects of Cu addition on the microstructure and properties of the Al–Mn–Fe–Si alloy. Journal of Alloys and Compounds, 2020, 834, 155175.	2.8	13
82	The characteristics of Cu–12wt.% Ag filamentary microcomposite in different isothermal process. Materials Science & Engineering A: Structural Materials: Properties, Microstructure and Processing, 2006, 418, 320-325.	2.6	12
83	Surface hardening of CrCoFeNi high-entropy alloys via Al laser alloying. Materials Research Letters, 2021, 9, 437-444.	4.1	12
84	FeS as a promising cathode catalyst for direct borohydride fuel cells. Journal of Alloys and Compounds, 2018, 769, 136-140.	2.8	11
85	Light-weight isometric-phase steels with superior strength-hardness-ductility combination. Scripta Materialia, 2018, 154, 230-235.	2.6	11
86	Laser cladding of layered Zr/Cu composite cathode with excellent arc discharge homogeneity. Surface and Coatings Technology, 2021, 421, 127454.	2.2	11
87	Nanocompound-induced anti-softening mechanisms: Application to CuCr alloys. Materials Science & Engineering A: Structural Materials: Properties, Microstructure and Processing, 2022, 841, 143038.	2.6	11
88	Grain boundary structure dependent fracture in nanocrystalline Au films. Materials Letters, 2011, 65, 2769-2771.	1.3	10
89	Dislocation assisted face-centered-cubic/body-centered-cubic interface mixing during severe plastic deformation. Journal of Alloys and Compounds, 2014, 586, 16-21.	2.8	10
90	Facile fabrication of a novel nanoporous Au/AgO composite for electrochemical double-layer capacitor. RSC Advances, 2015, 5, 38995-39002.	1.7	10

#	Article	IF	CITATIONS
91	Transmission electron microscopy observation of a deformation twin in TWIP steel by anex situtensile test. Philosophical Magazine, 2011, 91, 4033-4044.	0.7	9
92	FeS ₂ -sensitized ZnO/ZnS nanorod arrays for the photoanodes of quantum-dot-sensitized solar cells. RSC Advances, 2015, 5, 105324-105328.	1.7	9
93	Inhomogeneous ablation behaviors and failure mechanism of copper cathode in air. Science China Technological Sciences, 2020, 63, 2384-2394.	2.0	9
94	In situ study of the catalytic mechanism for the oxygen reduction reaction on a polypyrrole modified carbon supported cobalt hydroxide cathode in direct borohydride fuel cells. Physical Chemistry Chemical Physics, 2013, 15, 9070-9074.	1.3	8
95	A highly stable Cu(OH)2-Poly(vinyl alcohol) nanocomposite membrane for dramatically enhanced direct borohydride fuel cell performance. Journal of Power Sources, 2020, 467, 228312.	4.0	8
96	Influence of load orientations with respect to twin boundaries on the deformation behaviors of high-entropy alloy nanocrystals. MRS Bulletin, 2021, 46, 205-216.	1.7	8
97	Effect of Co addition on hardness and electrical conductivity of Cu–Si alloys. Journal of Materials Science, 2021, 56, 14821-14831.	1.7	8
98	Improvement of performance stability of electrolytic copper foils by bi-component additives. Journal of Applied Electrochemistry, 2022, 52, 1219-1230.	1.5	8
99	Enhanced plastic deformation capacity in hexagonal-close-packed medium entropy alloys via facilitating cross slip. Journal of Materials Science and Technology, 2023, 134, 1-10.	5.6	8
100	<i>In Situ</i> Study of Thermal Stability of Copper Oxide Nanowires at Anaerobic Environment. Journal of Nanomaterials, 2014, 2014, 1-6.	1.5	7
101	Cracking in a Fe–25Mn–3Si–3Al Steel. Materials Research Letters, 2014, 2, 204-208.	4.1	7
102	Synchrotron radiation <i>in situ</i> X-ray absorption fine structure and <i>in situ</i> X-ray diffraction analysis of a high-performance cobalt catalyst towards the oxygen reduction reaction. Physical Chemistry Chemical Physics, 2017, 19, 30749-30755.	1.3	7
103	Microstructure-Dependent Conformal Atomic Layer Deposition on 3D Nanotopography. Langmuir, 2012, 28, 15809-15815.	1.6	6
104	Unconventional Deformation Behaviours of Nanoscaled High-Entropy Alloys. Entropy, 2018, 20, 778.	1.1	6
105	Cold welding assisted self-healing of fractured ultrathin Au nanowires. Nano Express, 2020, 1, 020014.	1.2	6
106	Microstructure and properties of cold drawing Cu-2.5% Fe-0.2% Cr and Cu-6% Fe alloys. Journal of Zhejiang University: Science A, 2015, 16, 622-629.	1.3	5
107	In-situ TEM on the coalescence of birnessite manganese dioxides nanosheets during lithiation process. Materials Research Bulletin, 2016, 79, 36-40.	2.7	5
108	Predicting the property contour-map and optimum composition of Cu-Co-Si alloys via machine learning. Materials Today Communications, 2022, 30, 103138.	0.9	5

#	Article	IF	CITATIONS
109	Enhancing the ag precipitation by surface mechanical attrition treatment on Cu-Ag alloys. Metals and Materials International, 2016, 22, 831-835.	1.8	4
110	Deformation of Fe and Ag precipitates in Cu matrix. Materials Science & Engineering A: Structural Materials: Properties, Microstructure and Processing, 2016, 655, 86-91.	2.6	4
111	Bilayer Anion-Exchange Membrane with Low Borohydride Crossover and Improved Fuel Efficiency for Direct Borohdyride Fuel Cell. ACS Applied Materials & Interfaces, 2020, 12, 27184-27189.	4.0	4
112	Chromium, a promising cathode candidate for homogeneous arc erosion in air. Journal Physics D: Applied Physics, 2021, 54, 025304.	1.3	4
113	In situ study on stability of copper oxide nanomaterials by e-beam irradiation. Materials Letters, 2015, 156, 134-137.	1.3	3
114	Fuel permeability of anion exchange membranes under electric field. Electrochimica Acta, 2018, 266, 357-363.	2.6	3
115	Sustainable and homogeneous arc ablation behavior of zirconium cathodes improved by in situ formation of zirconium oxides. Journal Physics D: Applied Physics, 2021, 54, 245205.	1.3	3
116	The Effect of Heat Treatments on the Microstructural Evolution of Twin-Roll-Cast Al-Fe-Si Alloys. Journal of Materials Engineering and Performance, 2021, 30, 4401-4410.	1.2	3
117	EFFECT OF HEAVILY DRAWING ON THE MICROSTRUCTURE AND PROPERTIES OF Cu-Cr ALLOYS. Jinshu Xuebao/Acta Metallurgica Sinica, 2012, 48, 1459.	0.3	2
118	Nanofingers pulled from bulk silver. Scripta Materialia, 2012, 66, 247-249.	2.6	1
119	Enhancing Strength and Plasticity Synergy in Transformation-Induced Plasticity-Aided Lean Duplex Stainless Steel Based on the Ultrafine-Grained Austenite. Journal of Materials Engineering and Performance, 2022, 31, 2487-2495.	1.2	1
120	Extreme dislocation-mediated plasticity of yttria-stabilized zirconia. Materials Today Physics, 2022, 22, 100588.	2.9	1
121	Layer-by-layer laser cladding of crack-free Zr/Nb/Cu composite cathode with excellent arc discharge homogeneity. Surface and Coatings Technology, 2022, 444, 128653.	2.2	1
122	Influence of load orientations with respect to twin boundaries on the deformation behaviors of high-entropy alloy nanocrystals. MRS Bulletin, 0, , 1-12.	1.7	0
123	Laser Cladding Fe/FeCr Coatings on Continuous Casting Cu Mold. Advanced Engineering Materials, 0, , 2200653.	1.6	0